CFD Simulation of Vacuum Tower Feed Device Using the Two-Fluid Model

Paladino, E.E. [1]; Ribeiro, D. [2]; Reis, M. V. [2]; Geraldelli, W. [3]; Torres, G. [3]; Saito, A. [3] and Maliska, C. R. [1]

(1) SINMEC – Computational Fluid Dynamics Lab - Federal University of Santa Catarina, - Florianopolis - SC - Brazil. CEP: 88040-900
(2) ESSS – Engineering Simulation and Scientific Software – CELTA - Rod SC-401, Km001 - Florianopolis - SC – Brazil. CEP: 88030-000
(3) CENPES – PETROBRAS Research and Development Center - Cidade Universitaria Q.7 - Ilha do Fundao - Rio de Janeiro - RJ - Brazil. CEP: 21949-900

Prepared for Presentation at Topical Conference on Distillation AIChE 2003 Spring National Meeting, March 30 - April 3, New Orleans, Louisiana, at the session:
Refinery Distillation: Simple Modifications Yield Major Improvements

Unpublished

ABSTRACT

The aim of this work is to demonstrate the application of the two-fluid model (Eulerian Eulerian approach) for the flow analysis and geometry improvement of feed device and flash zone of a vacuum tower in a crude oil refinery. Initially, two-phase flow was calculated using the original geometry. Next, the patented enhanced Koch-Glitsch Vapor Horn® was simulated for geometry with two inlet devices and showed excellent performance in terms of vapor distribution and liquid entrainment. Pressure drop through the tower devices were in close agreement with operation values for the actual geometry. Results show the importance of using the Eulerian-Eulerian model in virtue of the influence of the liquid phase in the vapor phase flow pattern. Vapor vertical velocity and liquid volume fractions distributions are shown and compared for different feed nozzle geometries. Additionally the study also demonstrates the potential application of CFD tools for design and analysis of distillation columns.

Key words: numerical simulation, two-fluid model, vacuum tower, feed device, optimization

Introduction

The performance of a vacuum tower is greatly influenced by the flow pattern within the feed region. Therefore, the proper fluid dynamic design of the feed devices is of great importance for the column performance.

Recently, the CFD (Computational Fluid Dynamics) has become an essential tool to aid distillation column design, for feed devices and column internals as trays and structured beds as shown by van Baten and Krishna (2000), Soares *et al.* (2002), Mohamed Ali *et al.* (2001), and Laird *et al.* (2002), among others. It is possible to find various projects involving the numerical modeling of catalytic beds of reactive distillation (http://www.cpi.umist.ac.uk/intint/) and flow modeling in sieve trays (http://www-its.chem.uva.nl/research/cr). The use of CFD tools on distillation always had its bottleneck on hardware. This is because such models demand a huge computational load as a result of fine grids in a two-phase flow. Even with the latest hardware advances it is only feasible to run specific parts of the equipment.

The intention of this paper is to show the application of the two-fluid (Eulerian-Eulerian) model for the computation of the liquid-vapor flow within the flash zone of a vacuum tower in a crude oil refinery. This model takes into consideration the influence of the liquid phase flow in the vapor flow, once the presence of the liquid phase modifies the vapor vertical velocity distribution. Besides, this model gives much more information about the flow than the commonly used single-phase models or Eulerian-Lagrangian models. The Eulerian-Lagrangian model has the advantage over the single-phase model that they could predict qualitatively the liquid entrainment, however the two-fluid model predict additionally parameters such as liquid phase distribution, liquid velocity and phase interaction. In the Lagrangian model, the droplet motion is calculated considering the drag exerted by the continuous phase (vapor) but no interaction is considered from the droplets to the gas. For higher liquid volume fractions the velocity profile of the vapor phase is modified by the flow of liquid, as will be seen later in the results section.

Mathematical modeling

The two-fluid model was used to perform the simulations of the device. The governing equations of this model are obtained by an ensemble average of the Navier-Stokes equations for each phase and for the jump conditions, *i.e.*, the relations governing mass, momentum and energy transfer through the interface. The equations for mass and momentum conservation for each phase are:

$$\frac{\partial}{\partial t}(\rho_i)+\nabla(\rho_i \mathbf{U}_i)=0 \tag{1}$$

$$\frac{\partial}{\partial t}(\rho_i \mathbf{U}_i)+\nabla(\rho_i \mathbf{U}_i \mathbf{U}_i-\mathbf{T}_i)=\rho \mathbf{f}_i \tag{2}$$

And the jump conditions are given by:

$$\sum_j^k(\rho_i(\mathbf{U}_i-\mathbf{U}_I)\cdot\mathbf{n}_i)=0 \tag{3}$$

$$\sum_j^k(\rho_i(\mathbf{U}_i-\mathbf{U}_I)\mathbf{U}_i\cdot\mathbf{n}_i-\mathbf{T}_i\cdot\mathbf{n}_i)=\sigma\kappa\mathbf{n}_i \tag{4}$$

where k=i, j represent two contiguous phases and $\mathbf{U}_I$ is the interface velocity. These relations represent the mass and momentum transfer across the interface. In the case of momentum jump, the only imbalance of momentum across interface is given by surface tension, which is commonly neglected in dispersed flows. By dispersed flow we refer to particles in gas or liquid, bubbles in liquid, or droplets in gas. In this paper the droplets in gas was considered in the simulations.

In the case analyzed here, the problem was assumed isothermal, thus the energy equation is not included, but the hypothesis of one governing equation for each phase and a jump condition is applicable for any transported property.

Multiplying these equations by the phase indicator function defined as:

$$X_k(\mathbf{x},t)=\begin{cases}1 \text{ if } \mathbf{x} \equiv \text{ phase k at time t}\\ 0 \text{ otherwise}\end{cases} \tag{5}$$

and taking an ensemble average, the equations of the two-fluid model are obtained. These equations are given by:

$$\frac{\partial}{\partial t}(\rho r_i)+\nabla\cdot(\rho r_i\mathbf{U})=0 \tag{6}$$

$$\frac{\partial}{\partial t}(\rho r_i\mathbf{U}_i)+\nabla\cdot\left(\rho r_i\mathbf{U}_i\mathbf{U}_i-\left(\mathbf{T}_i+\mathbf{T}_i^{Turb}\right)\right)=-r_i\nabla p+r_i\mathbf{f}+\mathbf{M}_{il} \tag{7}$$

The averaging process is beyond the scope of this study and a detailed description can be found in Drew (1983) or Enwald *et al.* (1996).

The above equations represent the average flow of each phase and the interface. Like any averaging process, as the system becomes simpler to solve, some information is lost with respect to the flow and the interfacial phenomena, so that constitutive equations are needed. For single-phase systems, the problem lays on the turbulence modeling, which is reasonably well understood but for multiphase systems the problem of interface transfer arises and although this has generated a range of reports in the literature, it is still an open question.

In the above equations, the interfacial momentum transfer is represented by the term, $\mathbf{M}_{il}$. For the dispersed case the constitutive relations are obtained from the forces arising in a sphere, or deformed spheres in cases of bubbly flows, submerged in an accelerated external flow, as the relative velocity between phases. Therefore, the general form of this term is given by:

$$\mathbf{M}_{il}=\underbrace{C_D\rho_i A\left|\mathbf{U}_i-\mathbf{U}_j\right|\left(\mathbf{U}_i-\mathbf{U}_j\right)}_{Drag}+\underbrace{\rho_i r_j C_{VM}\left(\frac{D_j\mathbf{U}_j}{DT}-\frac{D_i\mathbf{U}_i}{DT}\right)}_{Virtual\ Mass}+$$
$$\underbrace{r_j\rho_i C_L\left(\mathbf{U}_i-\mathbf{U}_j\right)\left(\mathbf{U}_i\times\boldsymbol{\omega}\right)}_{Lift}+\frac{Other}{Forces} \tag{8}$$

By "other forces", we refer to forces of second order for the general case of multiphase flows. For a detailed description of the interfacial forces see Enwald & Peirano (1996), Kowe *et all* (1991), or Drew (1983). For low volume fractions of dispersed phase, as is the case of droplets in gas flows, the virtual mass and lift forces are negligible. Hence, the only interfacial force considered here was the drag. For this general situation, the model of Shiller Naumann is suitable. This is given by:

$$C_D=\max\left(\frac{24}{\mathrm{Re}}\left(1+0.15\,\mathrm{Re}^{0.687}\right),0.44\right) \tag{9}$$

where $\mathrm{Re} = \frac{\rho_G |\mathbf{U}_L - \mathbf{U}_G| d_L}{\mu_G}$ indicates the droplet Reynolds number.

The limit of 0.44 is included to represent the correct drag behavior, as droplet Re increase in some regions within the domain and may come into the inertial regime.

Model set-up

After the definition of the equations which govern the flow of each phase and the interface momentum transfer, the model set-up was made. The mass flow rates used for simulations were 40kg/s for the liquid phase and 30 kg/s for the vapor phase, giving a liquid volume fraction of 0.04 % at the domain inlet. Although these are realistic operational conditions for a vacuum tower of these characteristics, it was found that resulting absolute liquid entrainment (in kg/s, not in % of inlet mass flow) was too large. The explanation for this result is that the model considers the liquid phase as dispersed being more susceptible to be dragged to the upper region of the column, when actually a large part of the liquid phase remains stratified and falls down the column as a continuous phase. However, in this case the whole mass flow rate of liquid was considered dispersed, in order to show its influence on the vapor flow and highlight this feature of the Eulerian-Eulerian model. A good approximation for the real situation is to consider 10 to 15% of the liquid mass flow rate as dispersed phase only.

Figure 1 shows the investigated geometry and the computational grid. The model domain includes the inlet device, the flash zone, one collector and a slop wax bed, (illustrated in the figure) which was simulated as a porous media with a linear resistance.

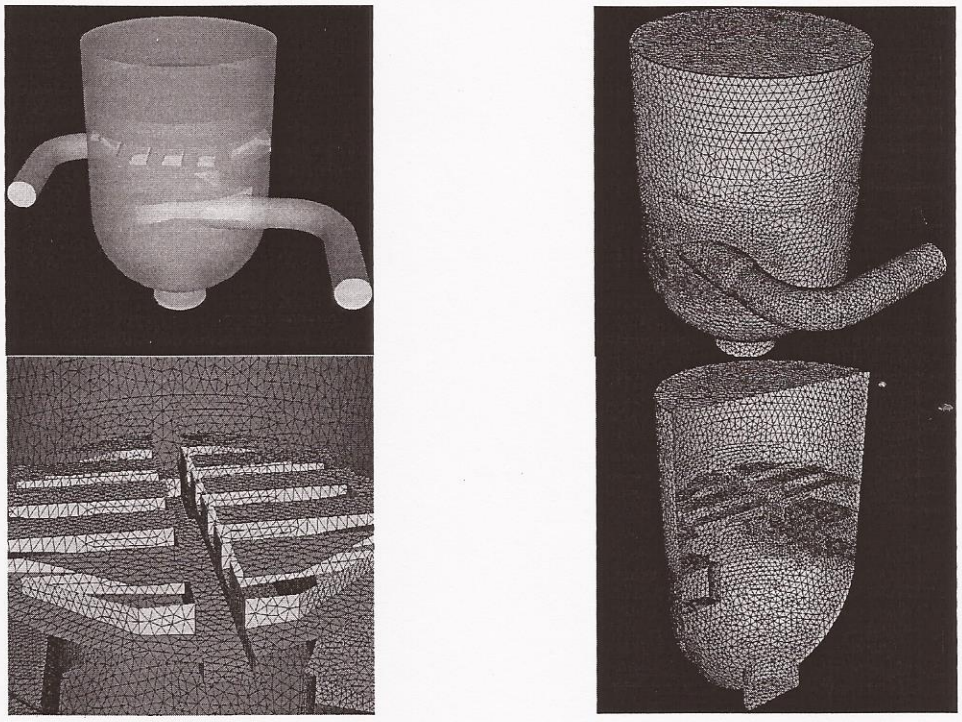

Figure 1 – Domain used in the simulations and computational grid details

The internal walls as well as collector and nozzle walls were simulated as thin surfaces, *i.e.*, internal walls with negligible thickness.

The tower bottom where liquid is withdrawn was simulated as a "degassing condition"[1] which acts as a wall for the continuous (vapor) phase and as an outlet for the dispersed (liquid) phase.

All the simulations were performed using the commercial code CFX-5.5. This code applies the Element Based Finite Volume Method ((Schneider and Raw (1987) and Maliska (2003))) for unstructured grids with a fully implicit coupled solver. This coupling includes mass and momentum equations and the phase coupling, *i.e.*, solves the whole system of equations for both phases simultaneously[1].

Results

This section will show some results obtained using the model described previously. Initially, results obtained with single phase and two-fluid model are compared for the original geometry in order to show the influence of the liquid phase on the vapor flow, mainly on the vapor distribution, which is of fundamental importance in the column performance. Next, another comparison is presented using the Koch-Glitsch Vapor Horn®, recently purchased by PETROBRAS. The objective of the present study is to evaluate the possible improvements within distillation process by the introduction of this feed device. It is important to mention that the Koch-Glitsch Vapor Horn® geometry was not changed in any way and the purpose of the study was to evaluate the vapor horn performance under different operational conditions. Results for both geometries are compared in terms of vertical vapor distribution and liquid entrainment.

For a more quantitative comparison the standard deviation of vapor vertical velocity is used. This approach to evaluate vertical vapor distribution was used by Mohamed Ali *et al.* (2001). The standard deviation of vertical vapor velocity, also called maldistribution factor is given by:

$$C_v = \left[\frac{1}{A_{Total}} \sum_{i=1}^{N} A_i \left(\frac{v_i - \bar{v}}{\bar{v}} \right)^2 \right]^{0.5} \tag{10}$$

where $\bar{v} = \frac{1}{A_{Total}} \sum_{i=1}^{N} A_i v_i$ is the area-averaged velocity within the referred plane.

Single and two-fluid models comparison

Figure 2 shows the velocity distribution at the nozzle center plane for the single phase and two-fluid model. At this location, great influence of the liquid phase in the vapor flow could be seen.

[1] See CFX–5 reference manual (2002)

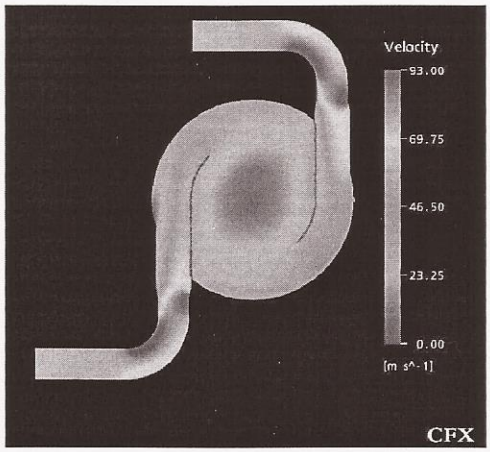

Single phase

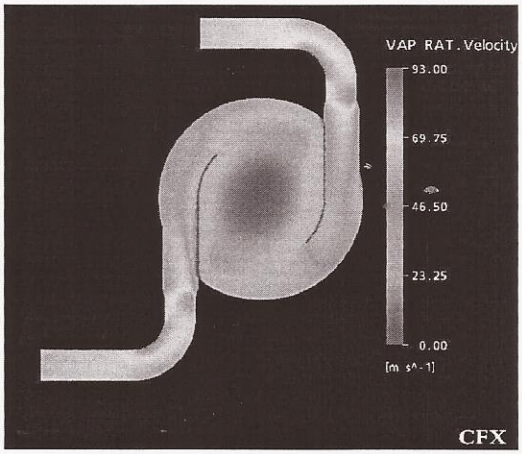

Two-Fluid Model

Figure 2 – Velocity distributions at nozzle center plane

Figure 3 shows the vapor vertical velocity distribution at a plane below the collector, for the single phase and two-fluid model as well as the C_v's for vertical velocity distribution.

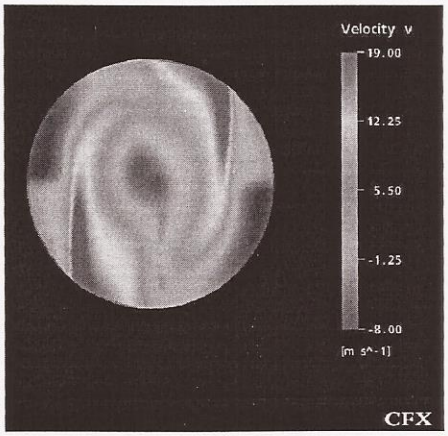

Single phase model vertical velocity – Cv = 2.1914

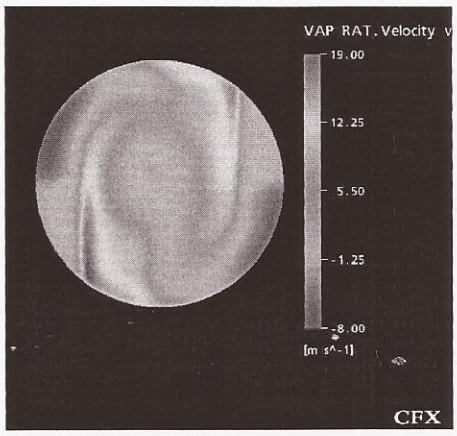

Two-Fluid model vertical velocity – Cv = 1.623

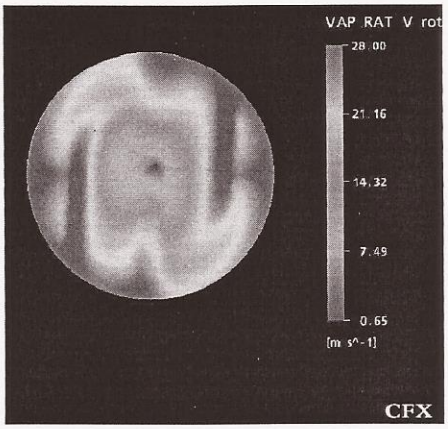

Single phase model rotational velocity

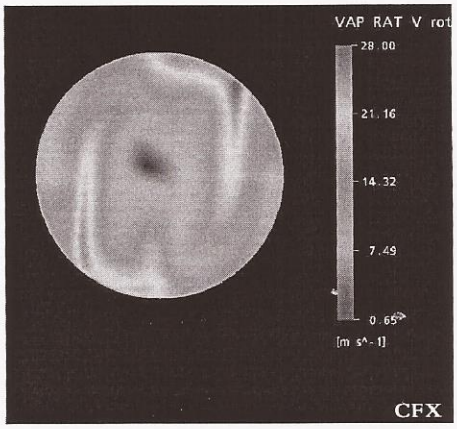

Two-Fluid model rotational velocity

Figure 3 – Velocity distributions at plane below collector

Figure 4 shows vertical and rotational vapor velocity distribution for a plane above collector.

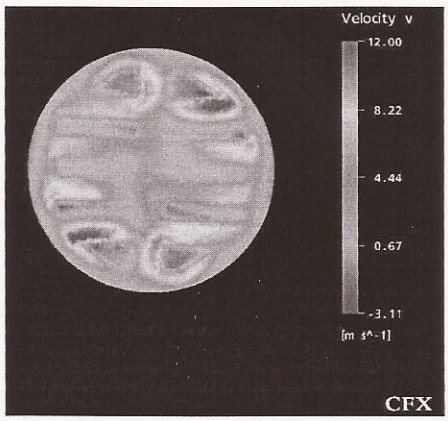

Single phase model vertical velocity – Cv = 0.85

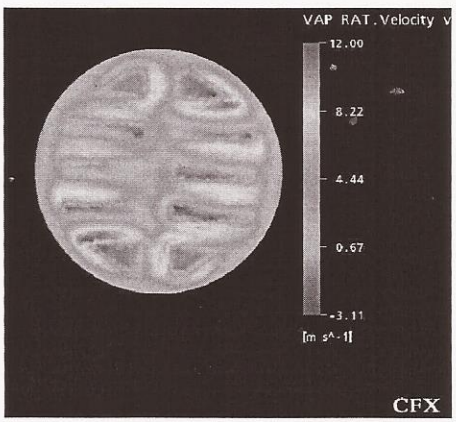

Two-Fluid model vertical velocity – Cv = 0.845

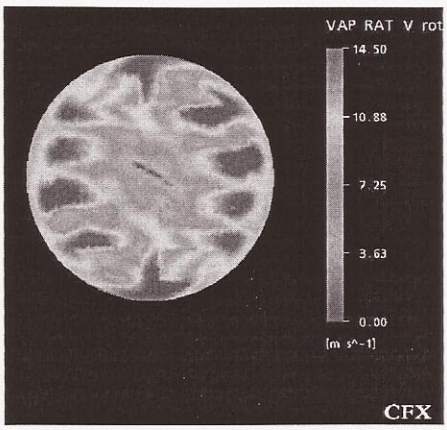

Single phase model rotational velocity

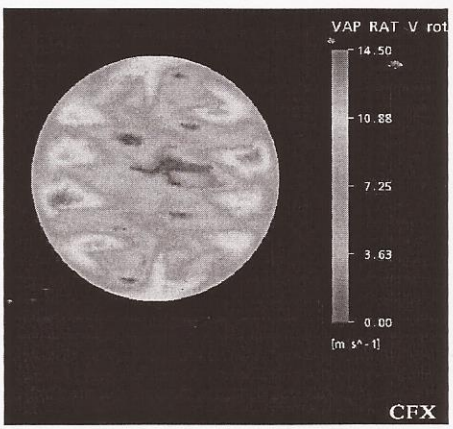

Two-Fluid model rotational velocity

Figure 4 – Velocity distributions at plane above collector

In general, results show that the liquid phase affects the vapor flow reducing its velocity and balancing out the vertical velocity distribution, as indicated in the C_v´s values. Hence, in many cases the vapor maldistribution and rotational velocities could be overestimated when using a single-phase model or a Eulerian-Lagrangian model, which does not consider the interaction between phases.

Furthermore, the Eulerian treatment of the dispersed phase allows calculating the phase distribution that is of fundamental importance in order to reduce liquid entrainment trough nozzle geometry modifications.

Figure 5 illustrates the liquid phase distribution along the column wall. It is possible to see a trend of liquid going down the column wall, however as can be seen in Figure 6, the feed line curvature makes liquid distribution at nozzle plane to be asymmetric. This kind of information is very valuable in order to improve the feed nozzle geometry.

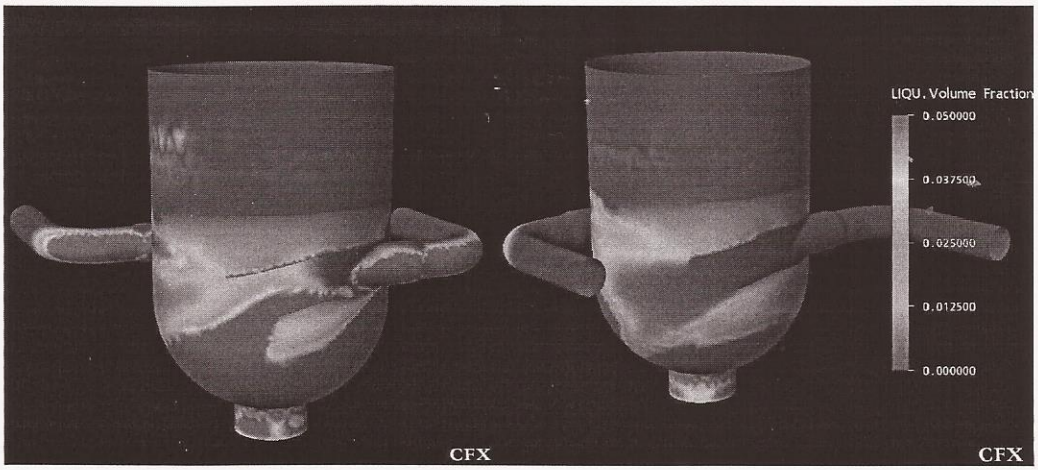

Figure 5 – Liquid phase distributions at the column wall

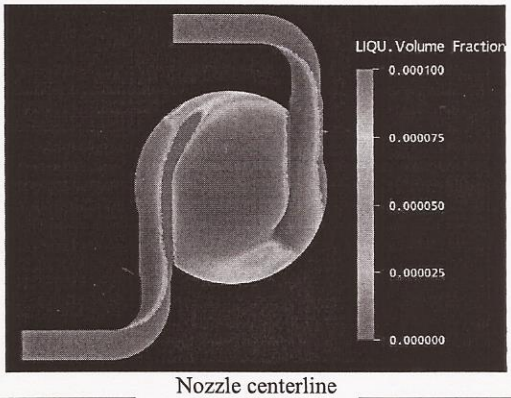

Nozzle centerline

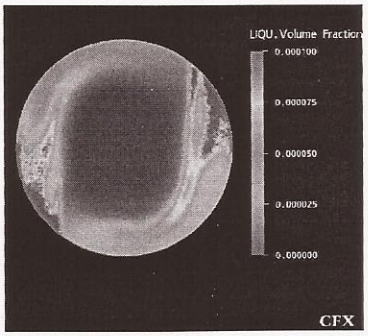

Below collector

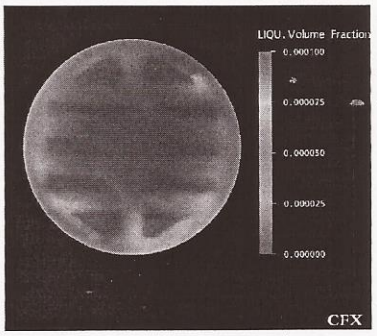

Above collector

Figure 6 – Liquid phase distributions at horizontal planes for the original feed nozzle

Comparison between original nozzle and Koch-Glitsch Vapor Horn®

In this section, the performance of original vapor horn and Koch-Glitsch Vapor Horn®, in terms of vapor distribution and liquid entrainment will be compared.

Figure 7 shows the computational grid for this geometry. The main characteristic of the Koch-Glitsch Vapor Horn® is the introduction of internal and external deflectors. The internal ones have

the purpose to drive the flow downward where a high intensity vortex will appear and the external deflectors will break this vortex improving the vapor distribution.

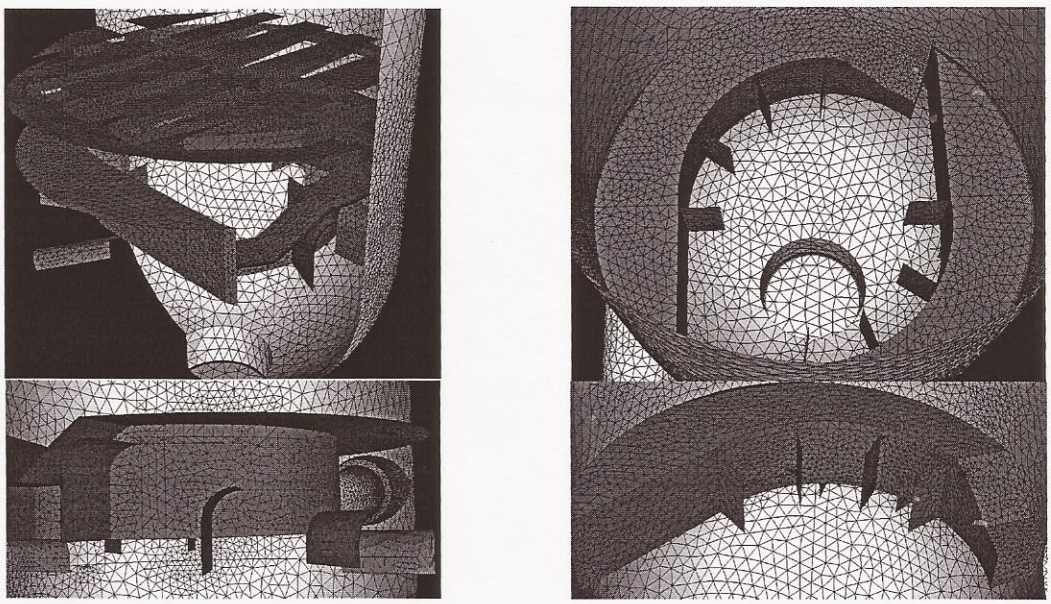

Figure 7 – Geometrical discretization of Kock-Glistsch Vapor Horn®

Figure 8 and Figure 9 show the vertical and rotational vapor velocity for the two geometries. It can be seen a great enhancement in terms of vertical velocity homogenization and reduction of rotational velocity. It is shown, for the plane below collector, an increase in C_v. This is mainly due to the increase in vertical velocity as a result to a decrease in rotational velocity. However, it can be seen a better large-scale distribution, since the standard deviation C_v, calculated using a plane mean velocity does not distinguish between large-scale and small-scale maldistribution (Mohamed Ali *et al.* (2001)).

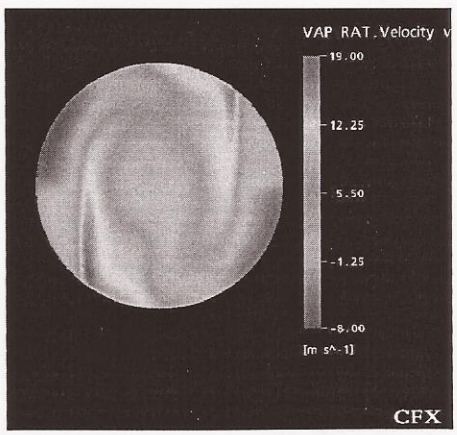

Original Vapor Horn vertical velocity – Cv = 1.623

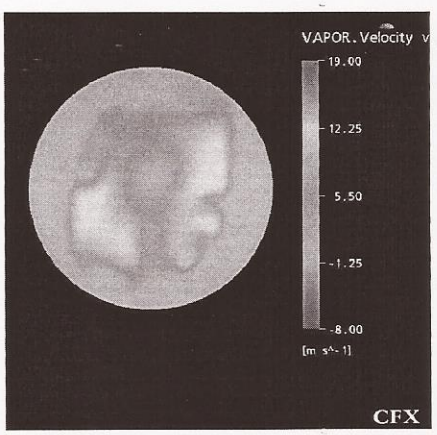

Kock-Glistsch Vapor Horn® vertical velocity – Cv = 1.145

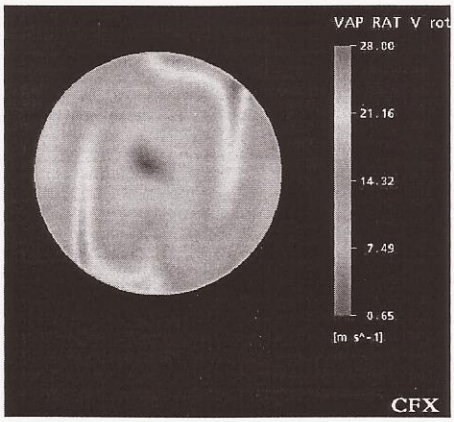

Original Vapor Horn rotational velocity

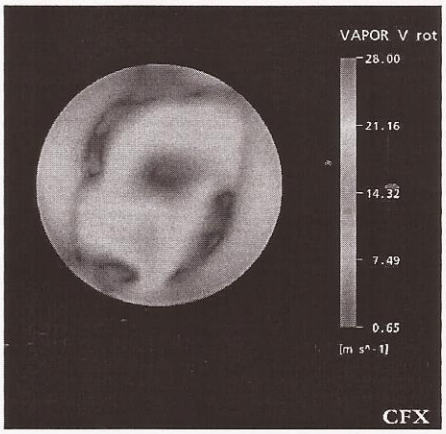

Kock-Glistsch Vapor Horn® rotational velocity

Figure 8 – Velocity distributions at plane below collector

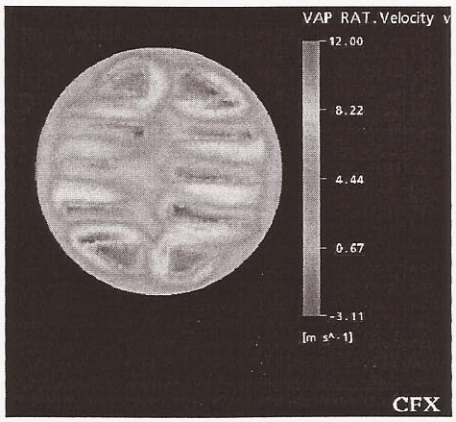

Original Vapor Horn vertical velocity – Cv = 0.845

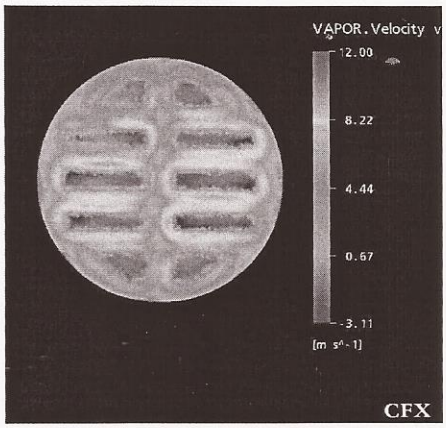

Kock-Glistsch Vapor Horn® vertical velocity – Cv = 0.94

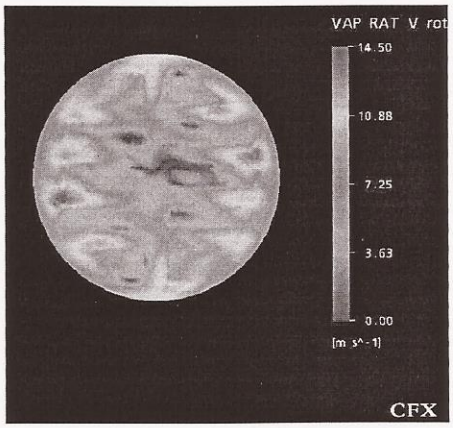

Original Vapor Horn rotational velocity

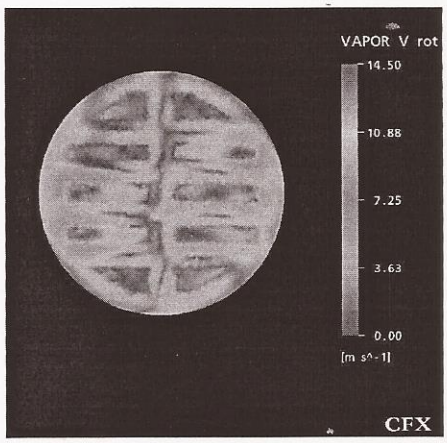

Kock-Glistsch Vapor Horn® rotational velocity

Figure 9 – Velocity distributions at plane above collector

Koch-Glitsch Vapor Horn® provides an improvement in terms of liquid entrainment. Figure 10 shows the liquid distribution at column wall for both nozzles.

It can be seen that for the Koch-Glitsch Vapor Horn® the liquid trend is to remain in the lower region of the column and the liquid entrainment is substantially reduced. Note that for the original case the liquid concentration at the wall remains high until the collector height and for the Koch-Glitsch Vapor Horn® the liquid is restricted to the lower region below the Vapor Horn.

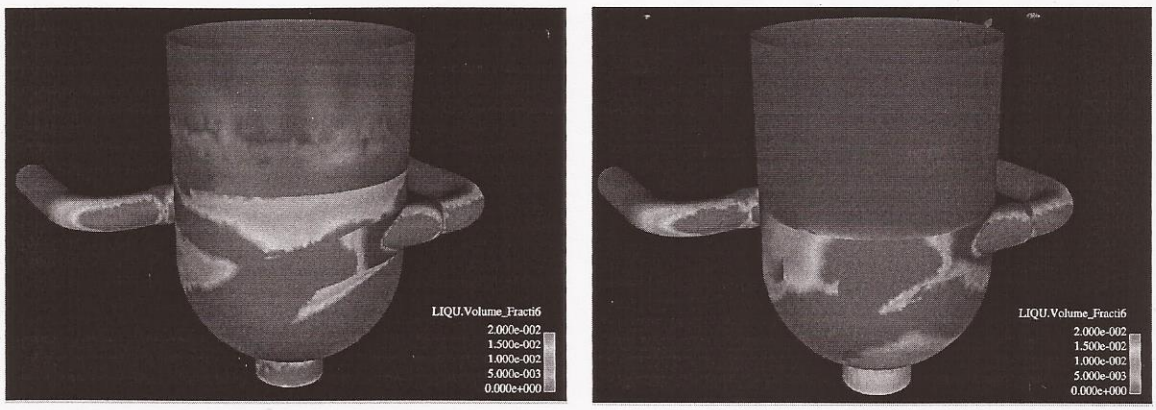

Original Vapor Horn Kock-Glistsch Vapor Horn®

Figure 10 – Liquid phase distributions at the column wall

Conclusions

The results presented in this study illustrates that the single phase modeling of the feed region could overestimate absolute velocities, rotational velocities and vapor heterogeneities. Besides, the two-fluid model allows estimating liquid entrainment and liquid distribution, which is of fundamental importance in order to introduce geometrical modifications that will result in less liquid entrainment. Lagrangian models could estimate qualitatively the fraction of liquid driven to the upper section of the column but it does not consider the influence of liquid phase on vapor flow. Moreover, it does not provide the liquid distribution along the computational domain since only a small fraction of liquid droplets trajectories can be calculated with the present hardware available.

In terms of geometry enhancement, the introduction of Koch-Glitsch Vapor Horn® improved the vapor distribution as well as a reduction in rotational velocities. Furthermore, liquid entrainment, which is strongly related to the vapor distribution, shows to be significantly reduced in comparison with original vapor horn.

Acknowledgements

This work was done with financial support of PETROBRAS S.A.

First author would like to thank Brazilian National Petroleum Agency (ANP) for the partial financial support through PRH-09.

Nomenclature

$\mathbf{U}_i$	Phase i velocity vector
r_i	Phase i volumetric fraction
ρ_i	Phase i mass density
$\mathbf{T}_i, \mathbf{T}_i^{Turb}$	Phase i viscous and Turbulent stress tensors
p	Pressure, shared by both phases
$\mathbf{M}_{il}$	Interfacial momentum transfer term
C_D, C_L, C_{VM}	Drag, Lift and Virtual Mass Coefficients
$\boldsymbol{\omega}$	Vorticity of continuous phase

References

1. CFX–5 Solver and Solver Manager Reference manual (2002) AEA Technology Engineering Software Ltd.
2. Drew, D. A. (1983) *Mathematical modeling of two-phase flows*, Annual Review of fluid mechanics, Vol. 15, pp 261-291
3. Enwald, H.; Peirano, E. and Almstedt, A. E. (1996) *Eulerian two-phase flow theory applied to fluidization*, Int. J. of Multiphase Flow, Volume 22, Supplement, pp 21–66.
4. Kowe, R; Hunt, J. C. R.; Hunt, A.; Couet, B. and Bradbury, L. J. S. (1988) *The effects of bubbles on the volume fluxes and pressure gradients in unsteady and non-uniform flow of liquids*, Int. J. of Multiphase Flows, Vol. 14, No. 5, pp 587-606.
5. Laird, D. Albert; B. and Schnepper, C. (2002) Optimization of Packed Tower Inlet Design by CFD Analysis, Proceedings of AIChE Spring National Meeting, New Orleans, LA, March 10 - 14
6. Maliska, C.R., (2003). *Numerical Heat Transfer and Fluid Flow*, 2nd edition, in Portuguese, in press, Livros Técnicos e Científicos Editora, Rio de Janeiro, Brazil.
7. Mohamed Ali, A.; Jansens, P. and Olujic Z. (2001) *The Use of Computational Fluid Dynamics to Model Gas Flow Distribution in Packed Columns*, Proceedings of the world congress of chemical engineering, Melbourne, Australia.
8. Schneider, G.E. and Raw, M.J.(1987) *Control-Volume Finite Element Method for Heat Transfer and Fluid Flow Using Co-located Variables – 1. Computational Procedure.*, Numerical Heat Transfer, Vol. 11, pp. 363-390
9. Soares, C; Noriler, D; Barros, A. A. C.; Meier, H.; Maciel, M. R. *Computational fluid dynamics for simulation of a gas-liquid flow on a sieve plate: model comparisons*. In: Distillation & Absorption 2002 - 634th Event of the European Federation of Chemical Engineering, Baden-Baden – Germany
10. van Baten, J.M. and Krishna, R. (2000) *Modeling sieve tray hydraulics using computational fluid dynamics*, Chemical Engineering Journal, Vol. 77, pp 143–151